JOURNAL OF GUIDANCE, CONTROL, AND DYNAMICS
Vol. 19, No. 3, May–June 1996

Dynamic Modal Truncation–Relaxation

S. Djerassi* and G. J. Iddan†
RAFAEL, Ministry of Defense, Haifa, Israel

Mechanical systems including elastic bodies are considered. When equations governing motions of such systems are generated, use is frequently made of the assumed-mode theory to describe elastic deflections of elastic bodies; and numerical integrations of these equations require an a priori determination of the number of modes being assumed. Here, a method called dynamic modal truncation–relaxation is introduced, whereby modes can be either truncated or relaxed at each integration step. The method is applied to a specific example, and a simulation code is constructed, showing that a significantly improved balance can be obtained between simulation efficiency (i.e., execution time) and simulation accuracy, as compared with the balance obtained with an a priori chosen number of modes. The method is useful when simulation run time is of importance, e.g., when real-time simulations are performed in the context of control design; when many simulations have to be performed in the context of a parameter study; or when missions of a long duration have to be simulated rapidly, as in the design of a new course for a spacecraft already in motion.

Introduction

EQUATIONS governing motions of systems with elastic bodies are frequently written with the aid of the assumed-mode theory, used to describe elastic deflections of elastic bodies.[1] When simulations of motions are performed by numerical integrations of the indicated equations, the number of modes is determined a priori, as in Refs. 2–7, representing in that regard a vast amount of literature. It turns out that the determination of the number of modes is not a simple matter. A large number of modes improves the accuracy of the simulation but lowers its efficiency. Indeed, the question of modal truncation was dealt with in the past, e.g., in Refs. 8 and 9. This question becomes especially important when violent events, such as ones associated with imposition of constraints, activation of control forces, or impacts, are involved. Under such circumstances, one may wish to accurately capture the dynamical behavior of the systems following the violent event, and needs, for that purpose, a large number of modes. Noting, however, that for its major part the motion involves no such events, and that the contribution of the higher modes dies out with time, one may find it desirable to delete those modes and improve the efficiency of the simulation.

In the present paper, a method called dynamic modal truncation–relaxation (DMTR) is introduced, whereby the number of modes can be changed during the simulation, i.e., at each integration step, from any current number to any other number. DMTR comes as an addition to other methods one may invoke to improve both the procedures leading to simulation codes and the efficiency of simulation of motion of dynamical systems. For example, one may use modal reduction techniques to improve modal-function generation (e.g., Guyan reduction, dynamic condensation[10]), one may argue about the best formulation for writing dynamical equations (e.g., Lagrange's equations, Newton–Euler equations, Kane's equations[11]), or one may employ methods to improve numerical integration of ordinary differential equations (e.g., Runge–Kutta methods, multistep methods[12]). Whatever methods one uses, however, one ultimately comes to grips with the question of how many modes to use in a particular case, and whether under the circumstances just described, this number can be changed during the simulation.

This paper refers only to this last question, introducing the DMTR method. The method is established in the following section, and is applied to a system representing a satellite carrying an elastic beam, after a heuristic truncation–relaxation criterion is set forth. A simulation code is constructed and run, showing that, with DMTR, a significant improvement is obtained in the accuracy of the simulation, as compared with one obtained by an a priori set small number of modes; and that a significant improvement is obtained in the simulation run time as compared with one obtained by an a priori set large number of modes.

Method

The method in question is based on the theory of imposition of constraints introduced in Ref. 13. The idea of imposition of constraints comes to light in connection with a holonomic system S of ν particles P_i $(i = 1, \ldots, \nu)$ of mass m_i, exerting contact forces on each other (but not on particles not belonging to S). The system possesses n generalized coordinates $q_1, \ldots, q_n$ and n generalized speeds $u_1, \ldots, u_n$ in N, a Newtonian reference frame, and undergoes three phases of motion as follows.

Phase A occurs in the time interval $0 \leq t \leq t_1$. The motion of S in N is defined as unconstrained and is governed by n dynamical equations, namely,

$$F_r + F_r^* = 0 \qquad (r = 1, \ldots, n) \tag{1}$$

where F_r and F_r^* are the rth generalized active force and the rth generalized inertia force, respectively.

Phase B is a transition phase that occurs in the time interval $t_1 \leq t \leq t_2$, where $t_2 - t_1$ is small, say, compared to time constants associated with the motion of S. During this phase, m constraints of the form

$$u_k = \sum_{r=1}^{p} C_{kr} u_r + D_k \qquad (k = p+1, \ldots, n) \tag{2}$$

are imposed on S, where

$$p \triangleq n - m \tag{3}$$

and C_{kr} and D_k are functions of $q_1, \ldots, q_n$ and time t. The configuration of S in N remains unaltered, that is,

$$q_r(t_2) = q_r(t_1) \qquad (r = 1, \ldots, n) \tag{4}$$

and the number of independent, generalized speeds is reduced from n to p. The relations between $u_k(t_2)$ $(k = p + 1, \ldots, n)$, the values of the dependent generalized speeds at $t = t_2$, and $u_r(t_2)$ $(r = 1, \ldots, p)$, the values of the independent generalized speeds at $t = t_2$, is given by

$$u_k(t_2) = \sum_{r=1}^{p} C_{kr} u_r(t_2) + D_k \qquad (k = p+1, \ldots, n) \tag{5}$$

Received July 27, 1994; presented as Paper 94-3574 at the AIAA Guidance, Navigation, and Control Conference, Scottsdale, AZ, Aug. 1–3, 1994; revision received Sept. 21, 1995; accepted for publication Nov. 15, 1995.

*Chief R&D Engineer, P.O. Box 2250.

†R&D Fellow, P.O. Box 2250.

Additionally, the relation between $u_s(t_2)$ $(s = 1, \ldots, n)$ and $u_s(t_1)$ $(s = 1, \ldots, n)$ is given by

$$\sum_{s=1}^{n}\left(m_{rs} + \sum_{k=p+1}^{n} C_{kr} m_{ks}\right)[u_s(t_2) - u_s(t_1)] = 0 \qquad (r = 1, \ldots, p) \quad (6)$$

where, with $\mathbf{v}^{P_i}$ as the velocity of P_i in N, m_{rs} is defined by

$$m_{rs} \triangleq -\sum_{i=1}^{\nu} m_i \frac{\partial \mathbf{v}^{P_i}}{\partial u_r} \frac{\partial \mathbf{v}^{P_i}}{\partial u_s} \qquad (r, s = 1, \ldots, n) \quad (7)$$

and where C_{kr}, D_k, and m_{rs} are evaluated at t_1.

Phase C occurs when $t > t_2$. Then the motion of S in N is defined as constrained and is governed by p dynamical equations, namely,

$$F_r + F_r^* + \sum_{k=p+1}^{n} C_{kr}\left(F_k + F_k^*\right) = 0 \qquad (r = 1, \ldots, p) \quad (8)$$

When phases A, B, and C occur in the reverse order, then S undergoes relaxation of constraints. The same equations govern this process, with t_1 and t_2 exchanging roles in Eqs. (4–6). Equations (4–6) imply that the linear and angular momentum of S at t_1 equal those at t_2. Finally, this formulation applies to simple, nonholonomic systems of n degrees of freedom if n in Eqs. (4) is replaced with $\bar{n}$, where $\bar{n} > n$.

Modal Truncation

In view of the theory just stated, dynamical modal truncation can be regarded as an imposition-of-constraints process. Thus, if m is the number of modes being truncated between t_1 and t_2, then the equations

$$u_k = 0 \qquad (k = p+1, \ldots, n) \quad (9)$$

play the role of Eqs. (2), and hence

$$C_{kr} = D_k = 0 \qquad (k = p+1, \ldots, n; \quad r = 1, \ldots, p) \quad (10)$$

(In the context of elastic deflections, $u_k \triangleq \dot{q}_k$, where q_k is the kth modal coordinate.) Consequently, Eqs. (5) and (6) reduce to

$$u_k(t_2) = 0 \qquad (k = p+1, \ldots, n) \quad (11)$$

and

$$\sum_{s=1}^{n} m_{rs}[u_s(t_2) - u_s(t_1)] = 0 \qquad (r = 1, \ldots, p) \quad (12)$$

and can be written in a matrix form, with $n \times n$ coefficient matrices, as follows:

$$\begin{bmatrix} m_{11} & \cdots & \cdots & \cdots & m_{1n} \\ \vdots & & & & \vdots \\ m_{p1} & \cdots & \cdots & \cdots & m_{pn} \\ \hline 0 & \cdots & 0 & & \\ \vdots & & \vdots & I & \\ 0 & \cdots & 0 & & \end{bmatrix} \begin{bmatrix} u_1(t_2) \\ \vdots \\ \vdots \\ \vdots \\ \vdots \\ u_n(t_2) \end{bmatrix} = \begin{bmatrix} m_{11} & \cdots & m_{1n} \\ \vdots & & \vdots \\ m_{p1} & \cdots & m_{pn} \\ \hline 0 & \cdots & 0 \\ \vdots & & \vdots \\ 0 & \cdots & 0 \end{bmatrix} \begin{bmatrix} u_1(t_1) \\ \vdots \\ \vdots \\ \vdots \\ \vdots \\ u_n(t_1) \end{bmatrix} \quad (13)$$

where I is the $m \times m$ identity matrix. In addition, Eqs. (8) reduce to

$$F_r + F_r^* = 0 \qquad (r = 1, \ldots, p) \quad (14)$$

which are the equations governing the motion of S after the truncation, with values for q_r $(r = 1, \ldots, n)$ and u_r $(r = 1, \ldots, n)$ at $t = t_2$ obtainable from Eqs. (4) and Eqs. (13), respectively. Note that $q_{p+1}(t_2), \ldots, q_n(t_2)$ appear in Eqs. (14), although the associated modes have been deleted. Accordingly, one can say that, if n' is the total number of modes, then the motion of S in N when $t > t_2$ is described with the aid of $n' - m$ active modes and m inactive modes.

Now, the modes being eliminated were the last m ones. Inspecting Eqs. (13) and (14), however, one may conclude that, in fact, any m modes can be deleted. To do so, one can replace Eqs. (13) and (14), respectively, with

$$\begin{bmatrix} 1 - e_1(t_2) + m_{11}e_1(t_2) & \cdots & m_{1n}e_1(t_2) \\ \vdots & & \vdots \\ m_{n1}e_n(t_2) & \cdots & 1 - e_n(t_2) + m_{nn}e_n(t_2) \end{bmatrix} \times \begin{bmatrix} u_1(t_2) \\ \vdots \\ u_n(t_2) \end{bmatrix} = \begin{bmatrix} m_{11}e_1(t_2) & \cdots & m_{1n}e_1(t_2) \\ \vdots & & \vdots \\ m_{n1}e_n(t_2) & \cdots & m_{nn}e_n(t_2) \end{bmatrix} \begin{bmatrix} u_1(t_1) \\ \vdots \\ u_n(t_1) \end{bmatrix} \quad (15)$$

and

$$\dot{u}_r[1 - e_r(t_2)] + \left(F_r + F_r^*\right)e_r(t_2) = 0 \qquad (r = 1, \ldots, n) \quad (16)$$

where $e_r(t_2)$ $(r = 1, \ldots, n)$ is a time-dependent variable having the value zero or one, depending on whether the rth mode becomes inactive at t_2 or not. The left-hand term on the left-hand side of Eqs. (16) is added so as to let $\dot{u}_r(t > t_2) = 0$ if $e_r(t_2) = 0$, which, together with $u_r(t_2) = 0$ obtained from Eq. (15), leads to

$$q_r(t > t_2) = q_r(t_2) = q_r(t_1) \quad (17)$$

in accordance with Eqs. (4). To summarize, Eqs. (1) and (15–17) govern the three phases associated with dynamic modal truncation.

Modal Relaxation

Suppose that m' modes are inactive when $t < t_1$, and that at $t = t_1$ their activation, or relaxation, is to be initiated. Then, with phases A, B, and C occurring in the reverse order, the equations

$$\dot{u}_r[1 - e_r(t_1)] + \left(F_r + F_r^*\right)e_r(t_1) = 0 \qquad (r = 1, \ldots, n) \quad (18)$$

govern the motion of S in N when $t < t_1$, and are replaced at $t = t_2$ by Eqs. (1). Here, $e_r(t_1)$ equals either one or zero, depending on whether the rth mode is active or not when $t < t_1$. Moreover, Eq. (15) has to be applied with t_1 and t_2 exchanging roles; hence

$$\begin{bmatrix} m_{11}e_1(t_1) & \cdots & m_{1n}e_1(t_1) \\ \vdots & & \vdots \\ m_{n1}e_n(t_1) & \cdots & m_{nn}e_n(t_1) \end{bmatrix} \begin{bmatrix} u_1(t_2) \\ \vdots \\ u_n(t_2) \end{bmatrix} = \begin{bmatrix} 1 - e_1(t_1) + m_{11}e_1(t_1) & \cdots & m_{1n}e_1(t_1) \\ \vdots & & \vdots \\ m_{n1}e_n(t_1) & \cdots & 1 - e_n(t_1) + m_{nn}e_n(t_1) \end{bmatrix} \times \begin{bmatrix} u_1(t_1) \\ \vdots \\ u_n(t_1) \end{bmatrix} \quad (19)$$

Next, suppose that the jth mode is relaxed between $t = t_1$ and $t = t_2$. Then, not only is the jth of Eqs. (1) restored, but also

$$u_j(t_2) = u_j(t_1) = 0 \quad (20)$$

Substitutions from m' such equations in Eqs. (19) lead to the following n-m' identities:

$$u_r(t_2) = u_r(t_1) \qquad (r \neq j) \tag{21}$$

Thus, Eqs. (18), (20), (21), and (1) indicate that dynamic modal relaxation involves the addition to the set of governing dynamical equations those equations associated with the relaxed modes and that the numerical values of all of the generalized speeds [and, in view of Eqs. (4), of all generalized coordinates] at $t = t_2$ equal those at $t = t_1$, respectively.

Simultaneous Modal Truncation–Relaxation

Suppose that m modes have to be truncated at $t = t_2$ in a system having m' inactive modes at $t = t_1$, where the two sets of modes may or may not intersect. A convenient way to proceed is to introduce an instant t' such that

$$t_1 < t' < t_2 \tag{22}$$

and let a total relaxation (i.e., of the m' inactive modes) occur between t_1 and t'. This means, in view of Eqs. (4), (20), and (21), that

$$q_r(t') = q_r(t_1) \qquad (r = 1, \ldots, n) \tag{23}$$

$$u_r(t') = u_r(t_1) \qquad (r = 1, \ldots, n) \tag{24}$$

and that Eqs. (18) are valid when $t < t_1$. Next, let m modes be truncated between t' and t_2. This means, in view of Eqs. (4) and (15), that

$$q_r(t_2) = q_r(t') \qquad (r = 1, \ldots, n) \tag{25}$$

$$\begin{bmatrix} 1 - e_1(t_2) + m_{11}e_1(t_2) & \cdots & m_{1n}e_1(t_2) \\ \vdots & & \vdots \\ m_{n1}e_n(t_2) & \cdots & 1 - e_n(t_2) + m_{nn}e_n(t_2) \end{bmatrix} \times \begin{bmatrix} u_1(t_2) \\ \vdots \\ u_n(t_2) \end{bmatrix} = \begin{bmatrix} m_{11}e_1(t_2) & \cdots & m_{1n}e_1(t_2) \\ \vdots & & \vdots \\ m_{n1}e_n(t_2) & \cdots & m_{nn}e_n(t_2) \end{bmatrix} \begin{bmatrix} u_1(t') \\ \vdots \\ u_n(t') \end{bmatrix} \tag{26}$$

and that Eqs. (16) are valid when $t > t_2$. Letting t_1 be the instant terminating a generic integration step, and t_2 be the instant starting the next step, one may summarize the DMTR formulation as follows. Equations (18) govern the motion of S when $t < t_1$; Eqs. (16) govern the motion of S when $t > t_2$;

$$q_r(t_2) = q_r(t_1) \qquad (r = 1, \ldots, n) \tag{27}$$

in view of Eqs. (23) and (25); and

$$\begin{bmatrix} 1 - e_1(t_2) + m_{11}e_1(t_2) & \cdots & m_{1n}e_1(t_2) \\ \vdots & & \vdots \\ m_{n1}e_n(t_2) & \cdots & 1 - e_n(t_2) + m_{nn}e_n(t_2) \end{bmatrix} \times \begin{bmatrix} u_1(t_2) \\ \vdots \\ u_n(t_2) \end{bmatrix} = \begin{bmatrix} m_{11}e_1(t_2) & \cdots & m_{1n}e_1(t_2) \\ \vdots & & \vdots \\ m_{n1}e_n(t_2) & \cdots & m_{nn}e_n(t_2) \end{bmatrix} \begin{bmatrix} u_1(t_1) \\ \vdots \\ u_n(t_1) \end{bmatrix} \tag{28}$$

in view of Eqs. (24) and (26). Each integration step terminates with the knowledge of $u_r(t_1)$ and $q_r(t_1)$ $(r = 1, \ldots, n)$, which are then used in Eqs. (27) and (28) to determine $u_r(t_2)$ and $q_r(t_2)$ $(r = 1, \ldots, n)$. These, in turn, serve as initial conditions for the next integration step.

Example

Shown in Fig. 1 is a system S moving in a planar orbit about E^*, the mass center of Earth, which is assumed to be fixed in N. The system S consists of a rigid body A and an elastic body B, assumed to behave as a Bernoulli–Euler cantilever beam attached to A at point $\bar{A}$. With two sets of three dextral, mutually perpendicular unit vectors $\boldsymbol{n}_j$ $(j = 1, 2, 3)$ and $\boldsymbol{a}_j$ $(j = 1, 2, 3)$, fixed in N and in A, respectively, the motion of S in N can be described as follows. Let $u_1, \ldots, u_{n+3}$ be $n + 3$ generalized speeds defined as follows:

$$u_1 \triangleq {}^N\boldsymbol{\omega}^A \cdot \boldsymbol{n}_3; \qquad u_{i+1} \triangleq {}^N\boldsymbol{v}^{A^*} \cdot \boldsymbol{n}_i \qquad (i = 1, 2) \tag{29}$$

$$u_{r+3} \triangleq \dot{q}_{r+3} \qquad (r = 1, \ldots, n) \tag{30}$$

where ${}^N\boldsymbol{\omega}^A$ and ${}^N\boldsymbol{v}^{A^*}$ are the angular velocity of A in N and the velocity of A^*, the mass center of A, in N, respectively; and let q_{r+3} be the rth modal coordinate used to describe the motion of B in A. The latter can be discussed in terms of y, the displacement in the $\boldsymbol{a}_2$ direction of a generic point of B, located in A so that the component of its position vector in the $\boldsymbol{a}_1$ direction is always x. In accordance with the assumed-mode theory, y is given by

$$y = \sum_{i=4}^{n+3} \phi_i(x) q_i \tag{31}$$

where ϕ_i $(i = 4, \ldots, n + 4)$, called modal functions, are chosen to be the ones associated with the solution of the partial differential equation governing the motion of B in A when A is fixed in N (Ref. 14) and when c, the coefficient of viscous friction, is zero. This equation reads

$$EJ\frac{\partial^4 y}{\partial x^4} + \rho\frac{\partial^2 y}{\partial t^2} + c\frac{\partial y}{\partial t} = 0$$

where EJ is the bending rigidity of B and ρ is the mass per unit length of B; and is subject to the following boundary conditions:

$$y(0) = y'(0) = y''(L) = y'''(L) = 0 \tag{32}$$

With I_{33}^A as the moment of inertia of A relative to A^* for $\boldsymbol{n}_3$, m_A and m_B as the masses of A and B, L as the length of B, and λ_i as the eigenvalue associated with ϕ_i, it is a straightforward matter to show that the generalized inertia forces for S in N are

$$F_1^* = -\left(I_{33}^A + m_B\frac{(a + L)^3 + a^3}{3L} + m_B\sum_{i=4}^{n+3} q_i^2\right)\dot{u}_1 + m_B z_1 \dot{u}_2 + m_B z_2 \dot{u}_3 - m_B \sum_{i=4}^{n+3}(aE_i + LF_i)\dot{u}_i - 2m_B u_i \sum_{i=4}^{n+3} q_i u_i \tag{33}$$

$$F_2^* = m_B z_1 \dot{u}_1 - (m_A + m_B)\dot{u}_2 + m_B \sum_{i=4}^{n+3} E_i \dot{u}_i s_1 - m_B z_2 u_1^2 + 2m_B u_1 \sum_{i=4}^{n+3} E_i u_i c_1 \tag{34}$$

$$F_3^* = m_B z_2 \dot{u}_1 - (m_A + m_B)\dot{u}_3 - m_B \sum_{i=4}^{n+3} E_i \dot{u}_i c_1 + m_B z_1 u_1^2 + 2m_B u_1 \sum_{i=4}^{n+3} E_i u_i s_1 \tag{35}$$

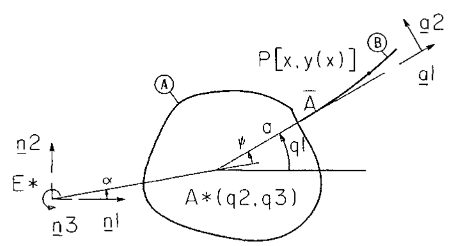

Fig. 1 Rigid body carrying an elastic beam.

$$F_i^* = -m_B(aE_i + LF_1)\dot{u}_1 + m_B E_i s_1 \dot{u}_2 - m_B E_i \dot{u}_3 - m_B \dot{u}_i + m_B u_1^2 q_i \qquad (i = 4, \ldots, n+3) \tag{36}$$

where

$$z_1 = \left(a + \frac{L}{2}\right)s_1 + \sum_{i=4}^{n+3} E_i q_i c_1$$
$$z_2 = -\left(a + \frac{L}{2}\right)c_1 + \sum_{i=4}^{n+3} E_i q_i s_1 \tag{37}$$

$$E_i = \frac{2}{L\lambda_i}\frac{\cos\lambda_i L + \cosh\lambda_i L}{\sin\lambda_i L + \sinh\lambda_i L}, \qquad F_i = \frac{2}{(\lambda_i L)^2} \tag{38}$$

$$s_1 \triangleq \sin q_1, \qquad c_1 \triangleq \cos q_1 \tag{39}$$

Furthermore, let $\boldsymbol{F}^P$ and $\boldsymbol{F}^A$ be the gravitation forces acting on an element dx located at P, a generic point of B, and on A, and let $\boldsymbol{M}^A$ be the gravitational moment acting on A. With

$$\Omega^2 \triangleq Gm_A/R_N^3, \qquad R_N^2 \triangleq q_2^2(0) + q_3^2(0) \tag{40}$$

where G is the universal gravitational constant; $\boldsymbol{F}^P$, $\boldsymbol{F}^A$, and $\boldsymbol{M}^A$ are given by

$$\boldsymbol{F}^P = -\Omega^2 \rho \mathrm{d}x \left(\frac{R_N}{|^N\boldsymbol{p}^P|}\right)^3 {}^N\boldsymbol{p}^P \tag{41}$$

$$\boldsymbol{F}^A = -\Omega^2 m_A \left(\frac{R_N}{|^N\boldsymbol{p}^{A^*}|}\right)^3 {}^N\boldsymbol{p}^{A^*} \tag{42}$$

$$\boldsymbol{M}^A = 3\Omega^2 \left(\frac{R_N}{|^N\boldsymbol{p}^{A^*}|}\right)^3 \cos\psi \sin\psi \left(I_{11}^A - I_{22}^A\right)\boldsymbol{n}_3 \tag{43}$$

Here, ${}^N\boldsymbol{p}^P$ and ${}^N\boldsymbol{p}^{A^*}$ are, respectively, the position vectors in N of points P and A^*, expressed as

$${}^N\boldsymbol{p}^P = q_2\boldsymbol{n}_1 + q_3\boldsymbol{n}_2 + (a + x)\boldsymbol{a}_1 + y\boldsymbol{a}_2 \tag{44}$$

and

$${}^N\boldsymbol{p}^{A^*} = q_2\boldsymbol{n}_1 + q_3\boldsymbol{n}_2 \tag{45}$$

Also (see Fig. 1)

$$\psi \triangleq q_1 - \tan^{-1}(q_3/q_2) \tag{46}$$

and I_{11}^A and I_{22}^A are the central principal moments of inertia of A for $\boldsymbol{a}_1$ and $\boldsymbol{a}_2$, respectively. Lastly, let $\boldsymbol{T} = T\boldsymbol{n}_3$ be an external torque acting on A. Then, linearized in x, the generalized active forces for S are

$$F_1 = 3\Omega'^2 q_2 \cos\psi \sin\psi \left(I_{11}^A - I_{22}^A\right) - m_b\Omega'^2 b_1 - cLa\sum_{i=4}^{n+4} E_i u_i - 2c\sum_{i=4}^{n+4} \lambda_i^{-2} u_i - T \tag{47}$$

$$F_2 = -m_A\Omega'^2 q_2 - m_B\Omega'^2 b_2 + cLs_1 \sum_{i=4}^{n+3} E_i u_i \tag{48}$$

$$F_3 = -m_A\Omega'^2 q_3 - m_B\Omega'^2 b_3 + cLc_1 + \sum_{i=4}^{n+3} E_i u_i \tag{49}$$

$$F_i = -cLu_i - EJLq_i\lambda_i^4 \qquad (i = 4, \ldots, n+3) \tag{50}$$

where

$$b_1 = (-q_2 s_1 + q_3 c_1)\left(a + \frac{-3a(a + q_2c_1 + q_3s_1)}{R_0^2}\right)\frac{L}{2} \tag{51}$$

$$b_2 = q_2 + ac_1\left(c_1 - \frac{3(q_2 + ac_1)(a + q_2c_1 + q_3s_1)}{R_0^2}\right)\frac{L}{2} \tag{52}$$

$$b_3 = q_3 + as_1 + \left(s_1 - \frac{3(q_3+as_1)(a+q_2c_1+q_3s_1)}{R_0^2}\right)\frac{L}{2} \tag{53}$$

and

$$\Omega'^2 = \Omega^2(R_N/R_0)^3, \quad R_0^2 = q_2^2 + q_3^2 + a^2 + 2a(q_2c_1 + q_3s_1) \tag{54}$$

The terms involving c in Eqs. (47–50) are associated with damping forces, and the last term in Eqs. (50) is associated with elastic forces. Substitution from Eqs. (33–36) and (47–50) in Eqs. (1) leads to the equations of motion of S in N.

Consider a motion of S with the following initial conditions:

$$q_1(0) = 0, \qquad q_2(0) = R_0, \qquad q_3(0) = 0$$
$$q_i(0) = 0 \qquad (i = 4, \ldots, n+3)$$
$$u_1(0) = \Omega, \qquad u_2(0) = 0, \qquad u_3(0) = \Omega R_0$$
$$u_i(0) = 0 \qquad (i = 4, \ldots, n+3)$$

and let a moment of $-3\boldsymbol{n}_3$ kg · mm be applied to A when $0.03 \le t \le 0.07$ s, and a moment of $3\boldsymbol{n}_3$ kg · mm be applied to A when $901.03 \le t \le 901.05$ s. We integrate the indicated equations of motion numerically, using one mode and six modes throughout the motion, with the following numerical values for the various parameters: $I_{11}^A = 0.1$, $I_{22}^A = 0.01$, $I_{33}^A = 0.01$ kg · mm · s^2; $m_A = 0.001$, $m_B = 0.0000468$ kg · mm^{-1} · s^2; $E = 21{,}000$ kg · mm^{-2}; $J = 20$ mm^4; $c = 10^{-7}$ kg · mm^{-2} · s. We obtain Fig. 2, which shows $y(L, t)$, the elastic deflection of the endpoint of B. Similarly, Fig. 3 shows $q_1(t)$, obtained with one mode and with six modes. Adopting the assumption that the larger the number of modes, the better the accuracy, one may refer to the curves obtained with six modes in Figs. 2 and 3 as benchmarks. One may then conclude that, whereas $q_1(t)$ can be predicted with reasonable accuracy with one mode, the elastic deflection cannot. The accuracy obtained with six modes does not come without price, however; a 910-s real-time simulation

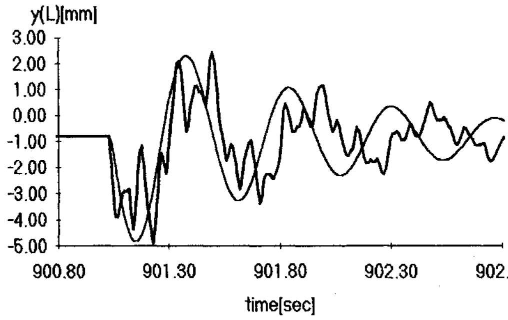

Fig. 2 $y(L, t)$ **without DMTR: ——, six modes and ——, one mode.**

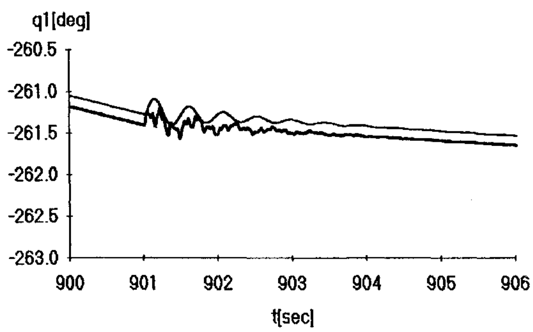

Fig. 3 $q_1(t)$ **without DMTR: ——, six modes and ——, one mode.**

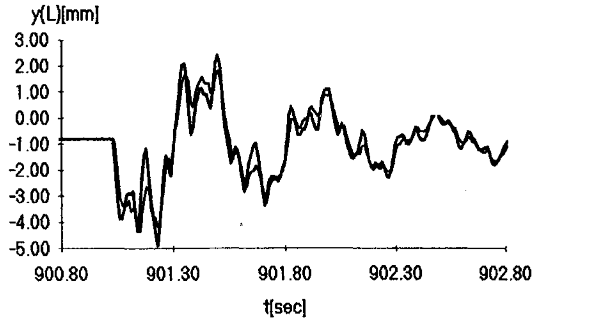

Fig. 4 $y(L,t)$: **—**, six modes without DMTR and —, six modes with DMTR.

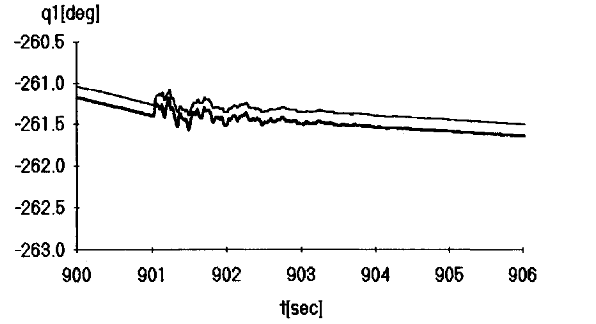

Fig. 5 $q_1(t)$: **—**, six modes without DMTR and —, six modes with DMTR.

takes 53 min to run on a 486 PC (with a Kutta–Merson integrator) with six modes, as compared with 22 min with the first mode.

A question arising at this point is this: can a better balance be obtained between the simulation efficiency and simulation accuracy? It will be demonstrated here that, even with a simple-minded truncation–relaxation criterion, a significantly improved balance can indeed be obtained, if use is made of the DMTR theory introduced in Sec. 2. For example, if one lets all the modes be active whenever $T \neq 0$, and lets the jth mode be truncated $7 - j$ s after T becomes zero, one obtains Figs. 4 and 5, with a 37-min simulation run time. A comparison of these figures with Figs. 2 and 3 reveals a significantly improved prediction of $y(L,t)$ as compared with the one obtained with the first mode.

With Eqs. (18) and (16) governing the motion of S when $t < t_1$ and when $t > t_2$, respectively, one may wonder whether a scheme simpler than that represented by Eqs. (27) and (28), for instance,

$$q_r(t_2) = e_r(t_2) q_r(t_1) \tag{55}$$

$$\begin{bmatrix} u_1(t_2) \\ \vdots \\ u_n(t_2) \end{bmatrix} = \begin{bmatrix} e_1(t_2) & 0 & \cdots & 0 \\ \vdots & & & \vdots \\ 0 & \cdots & 0 & e_n(t_2) \end{bmatrix} \begin{bmatrix} u_1(t_1) \\ \vdots \\ u_n(t_1) \end{bmatrix} \tag{56}$$

might lead to similar results. Figures 6 and 7 show $y(L,t)$ and $q_1(t)$ obtained with Eqs. (55) and (56) with the same truncation–relaxation criterion as before, the run time being 37 min. Whereas the two schemes in question give rise to the same $y(L,t)$ behavior, the latter leads to $q_1(t)$ that deviates appreciably from the one obtained with six modes. Thus, Eqs. (27) and (28) yield a tangible advantage over Eqs. (55) and (56).

An insight into the reason for this advantage can be gained with the aid of the following expressions:

$$\begin{aligned} \boldsymbol{H} = & \Bigg\langle \left(I_{33}^{A} + m_B(z_1 q_3 - z_2 q_2) + m_B \frac{(a+L)^3 - a^3}{3L} + m_B \sum_{i=4}^{n+3} q_i^2 \right) u_1 \\ & - [(m_A + m_B) q_3 - m_B z_1] u_2 + [(m_A + m_B) q_2 - m_B z_2] u_3 \\ & + m_B \sum_{i=4}^{n+3} [E_i (q_2 c_1 - q_3 s_1 + a) + L F_i] u_i \Bigg\rangle \boldsymbol{n}_3 \end{aligned} \tag{57}$$

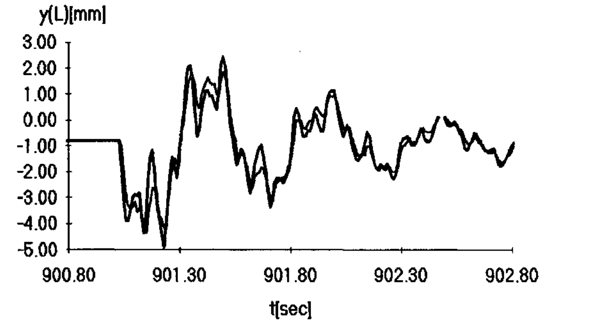

Fig. 6 $y(L,t)$: **—**, six modes without DMTR and —, six modes with simple DMTR.

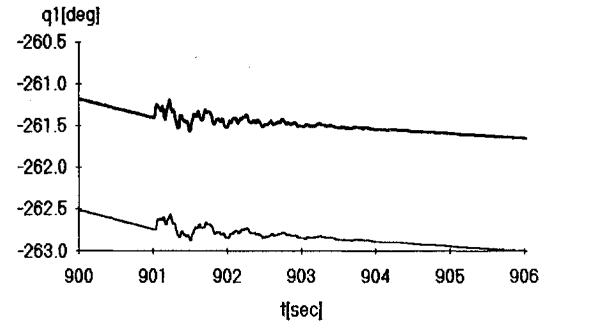

Fig. 7 $q_1(t)$: **—**, six modes without DMTR and —, six modes with simple DMTR.

$$\begin{aligned} \boldsymbol{L} = & \left(-m_B z_1 u_1 + (m_A + m_B) u_2 - m_B \sum_{i=4}^{n+3} E_i u_i \right) \boldsymbol{n}_1 \\ & + \left(-m_B z_2 u_1 + (m_A + m_B) u_3 + m_B \sum_{i=4}^{n+3} E_i u_i \right) \boldsymbol{n}_2 \end{aligned} \tag{58}$$

These are, respectively, the angular and linear momenta of S in N. Now, $e_r(t_2) = 1$ for $i = 1, 2$, and 3, because u_1, u_2, and u_3 defined in Eqs. (29) are associated with the motion of A in N. Identifying m_{rs} ($r = 1, 2, 3$; $s = 1, \ldots, n+3$) in Eq. (28) with the aid of Eqs. (33–36), one can show that

$$\boldsymbol{H} \cdot \boldsymbol{n}_3 = -\sum_{r=1}^{n+3} m_{1r} u_r + q_3 \sum_{r=1}^{n+3} m_{2r} u_r - q_2 \sum_{r=1}^{n+3} m_{3r} u_r \tag{59}$$

$$\boldsymbol{L} \cdot \boldsymbol{n}_1 = -\sum_{r=1}^{n+3} m_{2r} u_r, \qquad \boldsymbol{L} \cdot \boldsymbol{n}_2 = -\sum_{r=1}^{n+3} m_{3r} u_r \tag{60}$$

and that, in view of the three first rows of Eq. (28),

$$\boldsymbol{H}(t_2) = \boldsymbol{H}(t_1), \qquad \boldsymbol{L}(t_2) = \boldsymbol{L}(t_1) \tag{61}$$

The angular momentum and the linear momentum remain intact (only) during the imposition and/or relaxation phase, namely, between t_1 and t_2. Note that this need not be the case throughout the motion. In fact, this is not the case in the present example, since the system in question is subjected to gravity forces [Eqs. (41–43)].

One may associate with each generalized speed a contribution to the linear and angular momentum of S in N, and then regard Eqs. (27) and (28) as a formulation leading, when truncation–relaxation occurs, to a redistribution of the linear and angular momentum of S between the remaining contributors. This redistribution sheds light on the manner in which the simultaneous DMTR was handled; namely, the relaxation of all the inactive modes and subsequent truncation of those not meeting the survival criteria. Each of these relaxation–truncation steps leaves the linear and angular momentum intact between t_1 and t_2. By way of contrast, Eqs. (55) and (56) lead, upon truncation, to a loss of linear and angular momentum, and although the loss associated with each mode being truncated is small, its accumulated effect on the accuracy of the simulation is appreciable.

Further Exploitation

Precisely the same formulation used to carry out the DMTR, namely, that based on Eqs. (18), (16), (27), and (28), can be used to construct codes for the simulation of motions of systems undergoing changes in the number of degrees of freedom, when all of the constraint equations have the form of Eqs. (9). Examples of such systems are spacecraft deploying solar panels and booms, missiles deploying lift surfaces, etc. Taking a closer look at the former, suppose one wishes to investigate the attitude behavior of the spacecraft shown in Fig. 8 during the deployment of solar panels. The spacecraft consists of a main body S and of six panels A, B, C, D, E, and G, connected to S and to each other by revolute joints at points $\hat{S}$, $\hat{A}$, $\hat{B}$, $\bar{S}$, $\bar{D}$, and $\bar{E}$, and has a configuration characterized by $q_4, \ldots, q_9$. Initially, $q_4(0) = 270$ deg, $q_5(0) = 180$ deg, $q_6(0) = 180$ deg, $q_7(0) = 90$ deg, $q_8(0) = 180$ deg, and $q_9(0) = 180$ deg, whereas in the deployed configuration $q_4(t > t_4) = 360$ deg, $q_5(t > t_5) = 0$ deg, $q_6(t > t_6) = 360$ deg, $q_7(t > t_7) = 0$ deg, $q_8(t > t_8) = 360$ deg, and $q_9(t > t_9) = 0$ deg. Here, t_r $(r = 4, \ldots, 9)$ is the time at which the rth coordinate reaches the indicated value. Then the bodies associated with q_r are locked to each other (e.g., at t_4, S is locked to A, etc.). Torsion springs of constants k_A, k_B, k_C, k_D, k_E, and k_G are acting at points $\hat{S}$, $\hat{A}$, $\hat{B}$, $\bar{S}$, $\bar{D}$, and $\bar{E}$, respectively, exerting torques on two adjacent bodies directed so as to increase q_4, q_6, and q_8 and decrease q_5, q_7, and q_9. The equations governing the motion of the spacecraft can be constructed with the following definitions for generalized speeds:

$$u_r \triangleq {}^N\boldsymbol{w}^S \cdot \boldsymbol{s}_r \quad (r = 1, 2, 3) \qquad u_r \triangleq \dot{q}_r \quad (r = 4, \ldots, 9)$$

$$u_r \triangleq {}^N\boldsymbol{v}^{S^*} \cdot \boldsymbol{n}_{r+9} \quad (r = 1, 2, 3)$$

so that

$$^N\boldsymbol{w}^S = u_1\boldsymbol{s}_1 + u_2\boldsymbol{s}_2 + u_3\boldsymbol{s}_3$$

$$^N\boldsymbol{w}^4 = u_1\boldsymbol{s}_1 + u_2\boldsymbol{s}_2 + (u_3 + u_4)\boldsymbol{s}_3$$

$$^N\boldsymbol{v}^{S^*} = u_{10}\boldsymbol{n}_1 + u_{11}\boldsymbol{n}_2 + u_{12}\boldsymbol{n}_3$$

etc., where self-explanatory notation has been used. The constraints are $\dot{q}_r = 0$ $(r = 4, \ldots, 9)$, and the rth constraint is imposed at t_r. The derivation of the equations of motion and the implementation of Eqs. (18), (16), (27), and (28) in the context of a simulation code are straightforward, and will not be discussed any further.

Figure 9 shows u_3 during the deployment of panels from a spacecraft initially at rest [so that $u_r(0) = 0$, $r = 1, \ldots, 12$] with parameters that, with self-explanatory notation, have the following numerical values: $L = 1000$ mm, $m_S = 0.01$, $m_A = m_D = 0.00005$, $m_B = m_C = m_E = m_G = 0.0001$ kg · mm^{-1} · s^2; $I_1^S = 1600$, $I_2^S = 1500$, $I_3^S = 1340$, $I_{12}^S = 166$, $I_{13}^S = 150$, $I_{23}^S = 140$, $I_1^A = I_1^D = 4$, $I_2^A = I_2^D = 10$, $I_3^A = I_3^D = 2$, $I_1^B = I_1^C = I_1^E = I_1^G = 8$, $I_2^B = I_2^C = I_2^E = I_2^G = 16$, $I_3^B = I_3^C = I_3^E = I_3^G = 8$ kg · mm^{-1} · s^2; $k_A = 15$, $k_B = 40$, $k_C = 20$, $k_D = 25$, $k_E = 30$, $k_G = 10$ kg · mm/rad. Here, no external forces are exerted on the spacecraft; therefore the angular momentum of the spacecraft for S^* and the linear momentum in N are conserved. The theory of imposition of constraints[11] asserts that this is also the case during each of the impositions. Indeed, it has been verified that $|\boldsymbol{H}| = 0$ throughout the motion [note that $u_3(t > t_9) = 0$]. On the other hand, each of the generalized speeds undergoes an instantaneous change at t_r $(r = 4, \ldots, 9)$, affecting the orientation of S, and subjecting the spacecraft to a series of impacts. These effects can be minimized with a proper choice of system parameters, a choice that can be made expeditiously with the aid of a simulation such as the one in question.

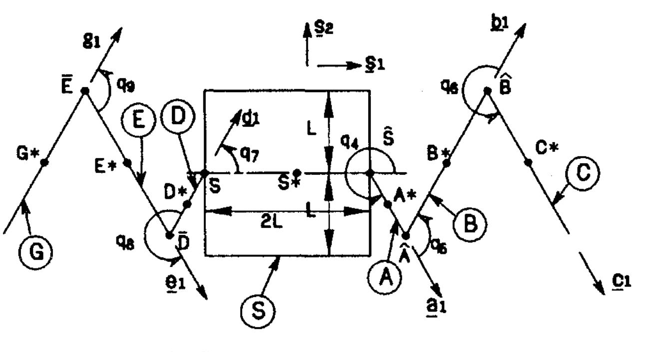

Fig. 8 Spacecraft deploying solar panels.

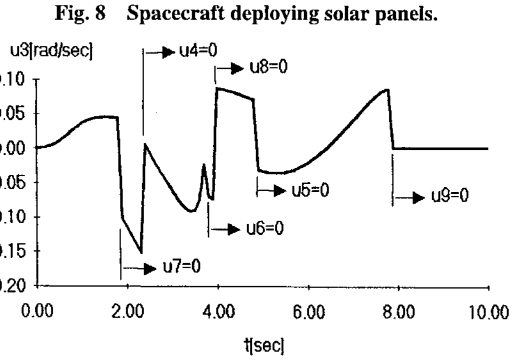

Fig. 9 $u_3(t)$ during deployment.

Conclusions

A method for DMTR was presented in connection with systems having flexible members, whose elastic behavior is described with the aid of modal representation. The largest number of modes to be used is determined a priori, and variables associated with each of the modes are tested against predetermined criteria at each integration step of the motion equations. Accordingly, modes are truncated, activated, or left intact. It was demonstrated that the method leads to results that are more accurate than those obtained with a single mode, on the one hand, and than those obtained with a simple modal truncation, on the other. The efficiency gained was moderate, but improves as the number of modes increases. The importance of the truncation–relaxation criterion in improving the balance between efficiency and accuracy cannot be overstated. Keeping, however, at least one mode active at all times, one cannot except to improve the simulation run time over whatever is obtained when a single mode is used throughout the simulation. The method in question comes into play independently of other methods [i.e., numerical methods, modal analysis methods and (dynamical) equation generation methods] used to improve the efficiency of dynamical simulations, or to improve the process leading to the underlying simulation codes.

References

[1]Meirovitch, L., *Analytical Methods in Vibrations*, Macmillan, London, 1967.

[2]Kane, T. R., and Ryan, R. R., "Dynamics of a Cantilever Beam Attached to a Moving Base," *Journal of Guidance, Control, and Dynamics*, Vol. 10, No. 2, 1987, pp. 139–151.

[3]Banerjee, A. K., and Dickens, J. M., "Dynamics of an Arbitrary Flexible Body in Large Rotation and Translation," *Journal of Guidance, Control, and Dynamics*, Vol. 13, No. 2, 1990, pp. 221–227.

[4]Buffinton, K. W., "Dynamics of Elastic Manipulators with Prismatic Joints," *Journal of Dynamic Systems, Measurement and Control*, Vol. 114/41, March 1992, pp. 41–49.

[5]Balas, M. J., "Low-Order Control of Linear Finite-Element Models of Large Flexible Structures," *Mechanics and Control of Large Flexible Structures*, edited by J. L. Junkins, Vol. 129, Progress in Astronautics and Aeronautics, AIAA, Washington, DC, 1990, pp. 295–313.

[6]Hughes, P. C., "Space Structure Vibration Modes: How Many Exist?," *IEEE Control Systems Magazine*, Feb. 1987, pp. 22–28.

[7]Baruh, H., and Choe, K., "Sensor Placement in Structural Control," *Journal of Guidance, Control, and Dynamics*, Vol. 13, No. 3, 1990, pp. 524–533.

[8]Likins, P. W., Ohkami, Y., and Wong, C., "Appendage Modal Coordinate Truncation Criteria in Hybrid Coordinate Dynamic Analysis," *Journal of Spacecraft and Rockets*, Vol. 13, No. 10, 1976, pp. 611–617.

[9]Hughes, P. C., and Sketon, P. E., "Modal Truncation for Flexible Spacecraft," *Journal of Guidance and Control*, Vol. 4, No. 3, 1981, pp. 291–297.

[10]Rao, S. S., *The Finite Element Method in Engineering*, Pergamon, Oxford, England, UK, 1989.

[11]Kane, T. R., and Levinson, D. A., "Formulation of Equation of Motion for Complex Spacecraft," *Journal of Guidance and Control*, Vol. 3, No. 2, 1980, pp. 99–112.

[12]Forsythe, G. E., Malcolm, M. A., and Moler, C. B., *Computer Methods for Mathematical Computations*, Prentice–Hall, Englewood Cliffs, NJ, 1977.

[13]Djerassi, S., "Imposition of Constraints," *Journal of Applied Mechanics*, Vol. 61, No. 2, 1994, pp. 434–439.

[14]Kane, T. R., Likins, P. W., and Levinson, D. A., *Spacecraft Dynamics*, McGraw–Hill, New York, 1983.